Journal of Non-Crystalline Solids 432 (2016) 183–188

Contents lists available at ScienceDirect

Journal of Non-Crystalline Solids

journal homepage: www.elsevier.com/ locate/ jnoncrysol

Electronic structure and photoluminescence properties of Zn-ion implanted silica glass before and after thermal annealing

D.A. Zatsepin [a,b], A.F. Zatsepin [b], D.W. Boukhvalov [c,d], E.Z. Kurmaev [a,b], Z.V. Pchelkina [a,d], N.V. Gavrilov [e]

[a] M.N. Miheev Institute of Metal Physics of Ural Branch of Russian Academy of Sciences, 18 Kovalevskoj Str., 620990 Yekaterinburg, Russia
[b] Institute of Physics and Technology, Ural Federal University, Mira Str. 19, 620002 Yekaterinburg, Russia
[c] Department of Chemistry, Hanyang University, 17 Haengdang-dong, Seongdong-gu, Seoul 133-791, Republic of Korea
[d] Theoretical Physics and Applied Mathematics Department, Ural Federal University, Mira Street 19, 620002 Yekaterinburg, Russia
[e] Institute of Electrophysics, Russian Academy of Sciences-Ural Division, 620016 Yekaterinburg, Russia

ARTICLE INFO

Article history:
Received 27 July 2015
Received in revised form 25 September 2015
Accepted 1 October 2015
Available online 22 October 2015

Keywords:
Phase transition;
Spectroscopy;
DFT modeling;
Doping

ABSTRACT

The results of XPS core-level and valence band measurements, photoluminescence spectra of a-SiO_2 implanted by Zn-ions (E = 30 keV, D = $1 \cdot 10^{17}$ cm^{-2}) and Density Functional Theory calculations of electronic structure as well as formation energies of structural defects in silica glass induced by Zn-ion implantation are presented. Both theory and experiment show that it is energetically more favorable for implanted zinc ions to occupy the interstitial positions instead of cation substitution. As a result, the Zn-ions embedded to interstitials, form chemical bonds with the surrounding oxygen atoms, fabrication ZnO-like nanoparticles and oxygen-deficient SiO_x matrix. The subsequent thermal annealing at 900 °C (1 h) strongly reduces the amount of ZnO nanoparticles and induces the formation of secondary α-Zn_2SiO_4 phase which markedly enhances the green emission.

1. Introduction

Embedding metal and semiconducting particles into SiO_2 host-matrix has been receiving considerable attention of materials scientists because it is a powerful method to re-build the electronic structure and physical properties of this practically significant wide-gap transparent insulator. Technological application of SiO_2 (both in crystalline and amorphous phases) actually is not limited with the use of only stoichiometric forms of silicon dioxide — also doped SiO_x (where $x < 2$) polymorphs are employed for passivation coatings and interlayers in microelectronics [1–2], low-index mid-infrared protecting coatings for mirrors [3], etc. Moreover, exactly embedded metal particles (MP) induce the nanostructuring of the silicon oxide and the major question arising herewith is linked with the final chemical state (formal valency) of MP's which will be fabricated by technological end-process treatment [4].

The most interest during last decades was focused on embedding Zn-metal particles into SiO_2 by means of Zn-ion implantation (see e.g. [4–8]). It is not surprising, because the understanding of Zn-ion incorporation process is the point for controlled modification of key electronic properties for SiO_2:Zn system that might be employed in the fields of photovoltaics, light-emitting/laser applications, optoelectronics, etc. An accumulated data reported previously [2–8] allow concluding that most of technologists are using thermal annealing in the range of temperatures from 600 °C up to 700 °C after Zn-ion embedding process in order to obtain the defect-free high-quality Zn-doped SiO_2. But these recent results seem far away from being perfect — i.e. Zn-implantation with 160 keV and 1.0×10^{17} cm^{-2} with the following 700 °C annealing did not display even the signs of Zn-incorporation into SiO_2-host [9]. The situation becomes better when 60 keV Zn-implantation of the same doze and 600 °C annealing had been applied, but in this case Zn-atoms are distributed non-uniformly and in the near surface region of SiO_2 substrate with partial oxidation of Zn-metal [5]. Also in the most of cited above papers the authors are concluding about significant transportation of Zn-atoms inside the volume of ion-beam treated host-matrix which is strongly impeding the high-quality uniformly nanostructured SiO_2:Zn fabrication.

In the present paper we have studied the electronic structure and luminescence properties of Zn-ion implanted silica glasses ($E = 30$ keV, $D = 1 \times 10^3$ cm^{-2}) before and after thermal annealing at 900 °C (1 h). The XPS measurements (core-levels and valence bands) are compared with performed density functional theory (DFT) calculations of the electronic density of states (DOS) and the formation energies for different configuration of structural defects that were induced by ion-implantation.

2. Experimental and calculations details

Silica glass samples of KU-type were implanted with Zn^+-ions having 30 keV energy with fluence of 1×10^{17} cm^{-2}. The KU-type of the glass is

E-mail address: danil@hanyang.ac.kr (D.W. Boukhvalov).

http://dx.doi.org/10.1016/j.jnoncrysol.2015.10.002
0022-3093/

a technological signature and means the high-purity optical silica glass of type III, obtained by hydrolysis technology from silicon tetrachloride vapor in oxygen-hydrogen flame. It has initially a high homogeneity, very low concentrations of metal impurities and high content of hydroxyl groups (the so-called "wet" silica glass). All these features provide a high radiation-optical stability and a high transparency in the UV and visible regions. Ion irradiation was performed employing the pulsed mode with pulse duration of 0.4 ms and frequency of 25 Hz. The current density of the beam during the pulse was not more than 0.6 mA/cm^2. Thermal annealing of the implanted samples was made at 900 °C in oxygen media within 1 h.

X-ray photoelectron spectroscopy (XPS) measurements were made with a PHI XPS Versaprobe 500 spectrometer (ULVAC-Physical Electronics, USA) allowing achieving an energy resolution of $\Delta E \leq 0.5$ eV for Al *Kα* radiation (1486.6 eV). As in our previous experiments, the samples under study were kept in 10^{-7} Pa vacuum for 24 h prior to measurement and then surface chemical state mapping attestation was made. Only samples whose surfaces were free from micro impurities were measured and reported herein. The XPS spectra were recorded using monochromatized Al *Kα* X-ray emission with the X-ray spot size of 100 μm in dia. The X-ray power load delivered to the sample was not more than 25 W in order to prevent X-ray stimulated sample decomposing. Under conditions mentioned, the typical XPS signal-to-noise ratios in our experiments were at least not worth than 10,000: 3. An experimental error for binding energy detection for described above conditions was not more than 0.15 eV according to the statement of XPS spectrometer manufacturer. Finally, the spectra were processed using ULVAC-PHI MultiPak Software 9.3 and then the residual background (BG) was removed using the Tougard approach with Doniach-Sunjic line-shape asymmetric admixture [10]. Well known, that most of the provided background models are self-consistent and they are using Doniach-Sunjic type of asymmetrical line-shapes that are acceptable in most common XPS cases. The advantage of retaining asymmetry in XPS data processing usually strongly apparent when a Tougaard BG is used in order to remove the extrinsic contribution to XPS-spectrum of a metal-like or metal-doped materials. Tougaard approach deals with a so-called "three-parameter universal cross-section" and has established values for a number of compounds, including aluminum and its oxides, silicon, silicon dioxide and others [10], so it is a theoretically based choice. After BG-subtraction, the XPS spectra were calibrated using reference energy of 285.0 eV for the carbon 1*s* core-level. Exactly such a sequence allows performing much better calibration due to previously removed outer contributions to the XPS line-shape.

An X-ray diffraction (XRD) measurements were made using an X'Pert Pro MRD X-ray diffractometer (Panalytical, Holland) under Cu *Kα* radiation with a 1° anticaster gap and a PIXcel detector having 3.347° of active length. The XRD patterns were recorded in a Bragg–Brentano parafocusing geometry with a nickel filter using the secondary beam.

Additionally the samples under study were certified with photoluminescence (PL) measurements. The photoluminescence spectra were recorded under selective excitation with 6.5 eV at room temperature using McPherson VUVAS 1000 PL spectrometer (McPherson, USA) with a 30 W deuterium light source. This system guaranteed meets the requirements of deep and vacuum ultraviolet analysis with the energy resolution of 0.2 eV and less than 0.5% of recorded PL-data distortion.

The electronic structures of SiO_2, Zn_2SiO_4 and Zn-doped SiO_2 were calculated using the tight-binding linear muffin-tin orbital (TB-LMTO) method [11–12] with the von Barth–Hedin local exchange-correlation potential [13]. The lattice constants and atomic positions corresponding to the $P3_121$ symmetry group of α-quartz were taken from Ref. [14]. The muffin-tin sphere radii were chosen to be $R(\mathrm{Si}) = 1.94$ a.u., $R(\mathrm{O}) = 1.6$ a.u. and 144 k points in the full Brillouin zone were employed for calculations. The simulation of the Zn defects (Zn(I) and Zn(S)) in the interstitial and in Si sites of α-quartz was performed with the super cell of 24 Si-atoms. The crystal structure data for the tetragonal phase of Zn_2SiO_4 with the space group *I*42*d* was taken from Ref. [15]. Here the muffin-tin sphere radii were chosen to be $R(\mathrm{Zn}) = 2.21$ a.u., $R(\mathrm{Si}) = 1.96$ a.u. and $R(\mathrm{O}) = 1.58$ a.u.: the 512 k points in the full Brillouin zone have been used for calculations. All the calculated DOSes are presented in Results and Discussion section.

Density functional theory (DFT) was also used for calculation of formation energies for different configurations of structural defects induced by Zn-ion implantation of *a*-SiO_2. These calculations were performed with using of the SIESTA pseudopotential code [16–19], a technique that has been recently successful in related studies of impurities in SiO_2 [18]. All calculations were made employing the Perdew–Burke–Ernzerhof variant of the generalized gradient approximation (GGA-PBE) [19] for the exchange-correlation potential. All calculations were made in spin-polarized mode. A full optimization of the atomic positions was carried out during which the electronic ground state was consistently found using norm-conserving pseudopotentials for the cores and a double-ξ plus polarization basis of localized orbitals for Si, Zn and O. The forces and total energies were optimized with accuracies of 0.04 eV Å^{-1} and 1.0 meV, respectively. Calculations of formation energies (E_{form}) were performed by considering the supercell both with and without a given defect [18]. For the current modeling of zinc impurity interactions with quartz-like matrix we used the $Si_{24}O_{48}$ supercell (see Fig. 1).

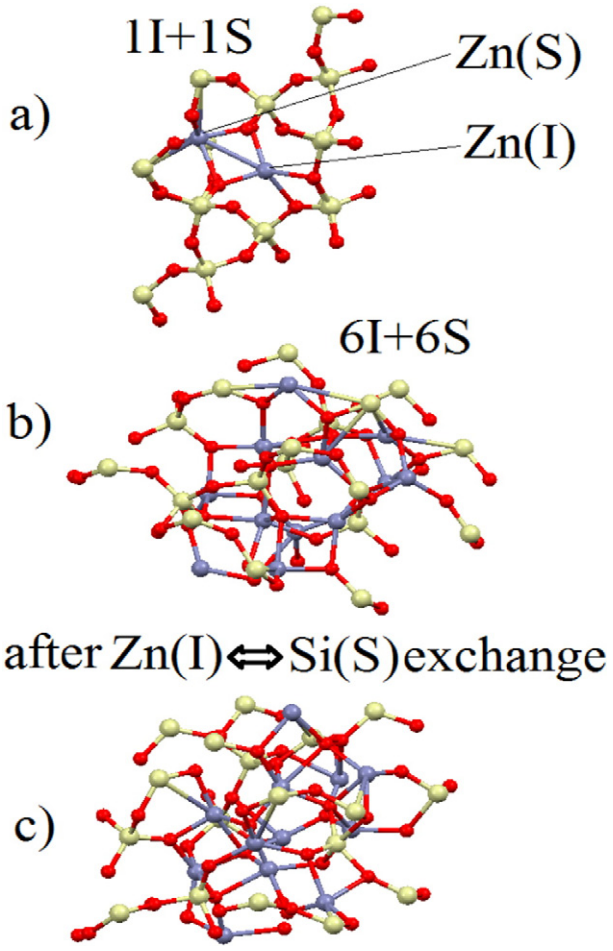

Fig. 1. (a) An optimized atomic structure of SiO_2 cluster at the first stage of ZnO-phase formation; (b) The very beginning of a ZnO-like cluster transformation to Zn_2SiO_4; (c) An exchange of interstitial Zn-impurity with Si from SiO_2 environment of ZnO-like cluster.